

## A Structure Determination of the Gluconate Ion\*

BY CECILY DARWIN LITTLETON

*The Institute for Cancer Research and The Lankenau Hospital Research Institute,  
Philadelphia 11, Pa., U.S.A.*

(Received 25 March 1953 and in revised form 27 April 1953)

Crystals of calcium, sodium, potassium and rubidium gluconates were investigated in order to determine the configuration of the gluconate ion,  $(C_6O_7H_{11})^-$ . The structure was determined by X-ray diffraction analysis of the last two, using the isomorphous-replacement method. Electron-density maps were calculated for the two projections,  $c$  and  $b$ . The crystal lattice data obtained were:

Sodium gluconate:  $a = 8.28$ ,  $b = 8.71$ ,  $c = 5.22$  Å,  $\beta = 104^\circ 42'$ ;  $P2_1$ ; 2 molecules.

Potassium gluconate:  $a = 23.63$ ,  $b = 7.46$ ,  $c = 5.05$  Å;  $P2_12_12_1$ ; 4 molecules.

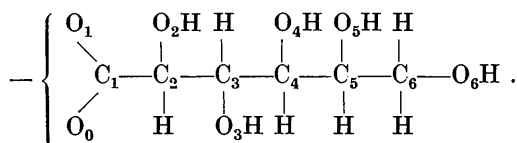
Rubidium gluconate:  $a = 23.94$ ,  $b = 7.52$ ,  $c = 5.63$  Å;  $P2_12_12_1$ ; 4 molecules.

The gluconate ion consists of a nearly planar six-membered zigzag carbon chain, with the seven oxygen atoms arranged above and below that plane. It bears a simple relation to  $\alpha$ -glucose.

In the potassium salt the potassium ions form parallel corrugated sheets throughout the crystal. Each potassium ion is coordinated to six oxygen atoms, four of them from four different carboxylate groups, and two from hydroxyl groups. Each carboxylate oxygen atom forms two ionic bonds to different potassium ions, and one hydrogen bond to a hydroxyl oxygen atom. Each hydroxyl oxygen atom forms two external bonds, generally hydrogen bonds to other oxygen atoms, and their hydrogen atoms are located in particular bonds. The molecular arrangement is such that there are columns, formed from pairs of gluconate ions in consecutive cells, running through the structure and firmly attached ionically to the potassium sheets.

### Introduction

In the degradation of glucose-6-phosphate to triose phosphate—a series of reactions important in the synthesis of pentose-5-phosphates for the nucleic acids—there is an oxidative pathway recently worked out by Cohen (1951), as well as the longer-established anaerobic Embden-Meyerhof scheme. Much of the argument for the mechanism of the oxidative pathway depends on the performance of gluconate or 6-phosphogluconate ion. Therefore the present research was undertaken to determine the configuration of the gluconate ion. The Fischer diagram is



Earlier work on lead gluconate gives no details of the structure of the gluconate residue other than that it is extended (Pepinsky, 1942).

### Experimental data

Gluconic acid is exceedingly hard to crystallize (Rehorst, 1928, 1930); consequently it was decided

to use the isomorphous-replacement method, employing the gluconates of either two alkali earth metals or two alkali metals.

*Calcium gluconate* (Merck's commercial) was found to be very soluble in water, crystallizing from it in clusters of fine white needles, which showed straight extinction between crossed nicols. However, when the crystals were removed from their mother-liquor they became soft and fragile and unsuitable for X-ray analysis.

*Sodium gluconate* was prepared by the neutralization of technical gluconic acid with strong sodium hydroxide solution. At first the addition of excess alcohol to the aqueous solution produced a syrup; but later, after standing for a week, hard chunky prisms with well developed faces were formed. Keenan & Weisberg (1929), using this method of crystallization, obtained crystals of no definite habit. However, their results agree with the writer's in that the crystals were anhydrous, showed straight extinction and were highly birefringent. Though the crystals of sodium and potassium gluconates showed very different habits, their stereographic projections had some similarities.

*Potassium gluconate* was prepared by neutralization at room temperature of technical gluconic acid with strong aqueous potassium hydroxide, using phenolphthalein as indicator. Five parts of 95% ethyl alcohol were added to the solution, and after a few hours white needles crystallized. In general their faces were not

\* This investigation was supported in part by a grant from the National Cancer Institute, National Institutes of Health, U.S. Public Health Service.

well developed. The crystals were hard and brittle, with no good cleavage plane. They were anhydrous and melted with decomposition at about 180° C. Between crossed nicols they showed straight extinction and a high birefringence. These data agree with the results of Keenan & Weisberg (1929) for potassium gluconate.

*Rubidium gluconate* was prepared by the double decomposition of barium gluconate and rubidium sulphate (Keenan & Weisberg, 1929). Barium gluconate was obtained by boiling technical gluconic acid with a slight excess of barium carbonate for an hour, letting it cool, and filtering off the excess carbonate. Then rubidium sulphate solution was added drop by drop from a separating funnel to the boiling barium gluconate solution. When cool, the barium sulphate was filtered off, and to the filtrate were added ten parts of alcohol. Long white needles separated after a few hours. They were similar to the potassium gluconate crystals in physical and optical properties but were better developed.

### X-ray data

Weissenberg and precession photographs, using nickel-filtered copper  $K\alpha$  radiation, were taken of sodium gluconate. They showed the crystals to be monoclinic, space group  $P2_1$ , having two molecules in a cell of dimensions:

$$a = 8.28, b = 8.71, c = 5.22 \text{ \AA}, \beta = 104^\circ 42'.$$

The length of the unique symmetry axis suggested that the structure determination would be difficult, and the work was concluded at this point.

Crystals of potassium gluconate, and later of rubidium gluconate\*, were mounted to rotate about the needle axis  $c$ , and the  $b$  axis, and were photographed under the conditions described above. The photographs showed that the two substances are isomorphous and have orthorhombic symmetry. The systematic absence of  $h00$ ,  $0k0$  and  $00l$  for  $h$ ,  $k$  or  $l$  odd shows that the space group is  $P2_12_12_1$ , with four asymmetric units per cell. The cell dimensions are:

Potassium gluconate,  $a=23.63$ ,  $b=7.46$ ,  $c=5.05 \text{ \AA}$ .  
 Rubidium gluconate,  $a=23.94$ ,  $b=7.52$ ,  $c=5.63 \text{ \AA}$ .

The calculated density of potassium gluconate, assuming four molecules per cell, is  $1.74 \text{ g.cm.}^{-3}$ , in close agreement with the observed value of  $1.73 \text{ g.cm.}^{-3}$ .

To obtain relative intensities the usual multiple-film technique was employed. The intensities were estimated visually by comparison with a logarithmic scale and corrected for Lorentz and polarization factors. The 200 reflection has a reciprocal spacing too

short to appear on the Weissenberg films, and it was obtained with some difficulty from oscillation photographs taken on a Unicam X-ray goniometer.

### Structure determination

Patterson maps (1934, 1935) of the potassium gluconate structure projected down the  $c$  and  $b$  axes were calculated, but they gave no indication of the position of the potassium ion. When the Patterson projection of the rubidium salt down the  $c$  axis had been calculated, it was compared with that of the potassium salt, and the position of the heavy atom immediately became apparent. From this the signs of most of the  $hk0$  reflections of the rubidium salt were determined, and, using these terms, the electron-density map was calculated. Calculation of all Fourier series was carried out using Patterson & Tunell's method (1942), in 60ths of the cell edges.

A model of the gluconate ion consistent with E. Fischer's convention was made of rubber balls joined by plastic rods. In the model, as in the molecule, there was free rotation about the C-C bonds, which allowed it to be twisted so as to give the best possible interpretation of the map of the electron-density projection. By this method  $x$  and  $y$  coordinates were found for the carbon and oxygen atoms; structure factors were calculated, and another refinement of the electron-density projection was undertaken. This second  $c$ -axis map of the rubidium salt showed much greater resolution of atomic positions and confirmed the correctness of the chosen configuration of the gluconate ion.

The refinement of the structure was now continued with potassium gluconate. Its structure factors are more sensitive to the coordinates of the light atoms than are those of the rubidium salt. Two refinements of the  $c$ -axis projection were made before work was started on the  $b$ -axis projection.

Even knowledge of the  $x$  coordinate of the potassium ion on the Patterson map of the  $b$ -axis projection did not reveal its  $z$  coordinate. However, a very rough calculation of a strip of the corresponding map of rubidium gluconate showed the  $z$  coordinate of the heavy atom. The signs determined by the position of the rubidium atom were then allocated to some of the terms in the Fourier series for potassium gluconate. When the electron-density map had been obtained, the model of the gluconate ion, without alteration, was fitted as well as possible to it, bearing in mind the  $x$  coordinates of the atoms obtained from the  $c$ -axis projection. Two refinements were carried out, during which the resolution greatly improved. After that the projection was correlated with the  $c$ -axis projection and the first set of bond lengths calculated. The less well resolved carbon atoms were given coordinates consistent with reasonable bond lengths for C-C and C-O, and a further refinement of each map was undertaken. No calculation was made for the bond

\* I wish to thank Mrs Joan R. Clark and Mrs Alice Sword Weldon for taking the excellent photographs of rubidium gluconate, and also for help with the calculations.

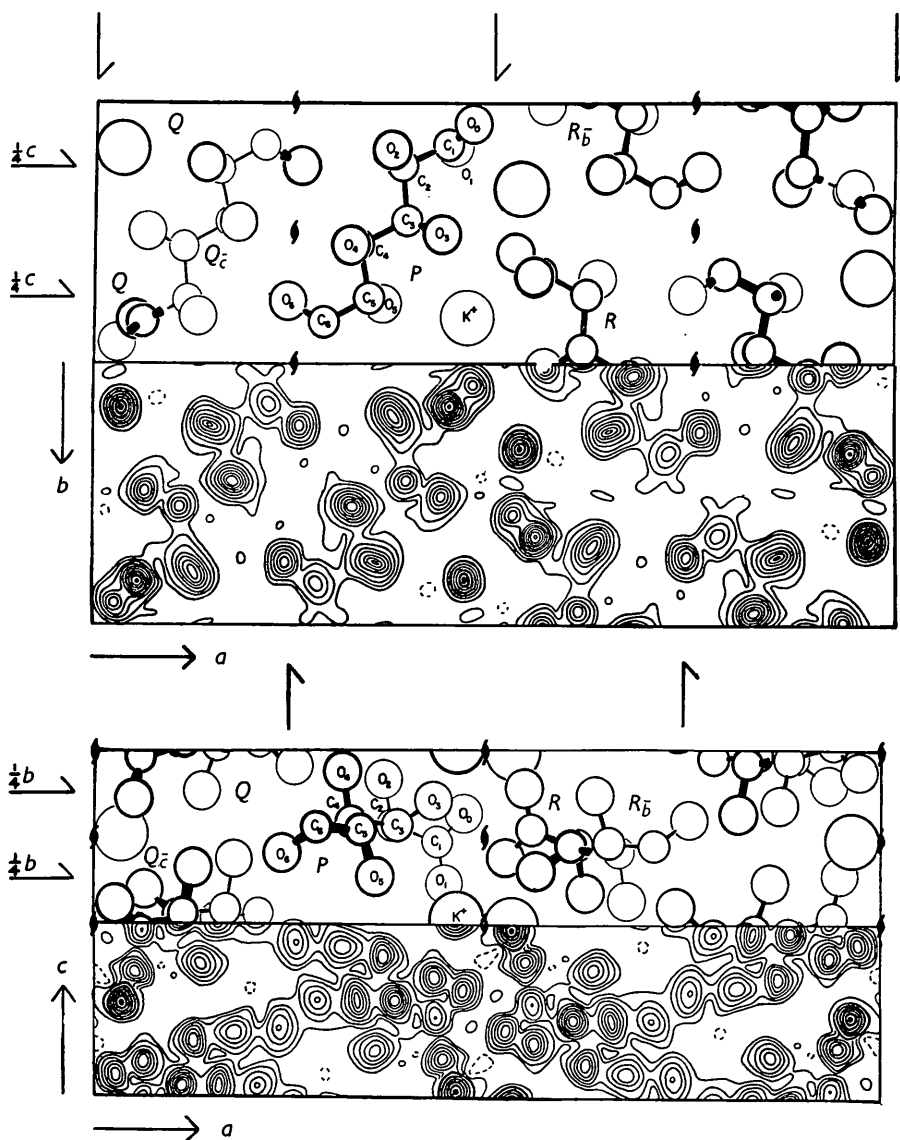


Fig. 1. The lower cell shows the electron density of potassium gluconate projected down the  $c$  axis. The upper cell shows the arrangement of the molecule in this projection. Contours are drawn at  $1 \text{ e.}\text{\AA}^{-2}$ ,  $2 \text{ e.}\text{\AA}^{-2}$ , and after that at intervals of  $2 \text{ e.}\text{\AA}^{-2}$ , except on the potassium ion where they are drawn at  $1 \text{ e.}\text{\AA}^{-2}$ ,  $5 \text{ e.}\text{\AA}^{-2}$ , and after that at intervals of  $5 \text{ e.}\text{\AA}^{-2}$ . The broken contour represents  $-1 \text{ e.}\text{\AA}^{-2}$ .

Fig. 2. The lower cell shows the electron density of potassium gluconate projected along the  $b$  axis. The upper cell shows the arrangement of the molecule. Contours are the same as in Fig. 1. (For simplicity  $\text{O}_3$  is given to  $R$  instead of  $R_{\bar{5}}$ .)

angles at this stage. This process of refinement was repeated once more, giving the final atomic coordinates listed in Table 1. The final map of the electron-density projection down the  $c$  axis is shown in Fig. 1, and that down the  $b$  axis in Fig. 2.

The origin of both maps lies on the  $b$  screw axis in the perpendicular plane containing the  $c$  screw axes. Only molecule  $P$  lies completely within the cell; the other molecules are derived from it by the operations of the space group. The  $c$  screw axis at  $\frac{1}{4}a$  (Fig. 2), operating on  $P$  in a positive direction, gives rise to molecule  $Q$ ,  $\frac{1}{2}c$  upwards; the equivalent molecule in the cell below is  $Q_{\bar{c}}$ .  $P_c$  is in the cell above. The  $b$  screw

axis at  $\frac{1}{2}a$  (Fig. 1), operating on  $P$  in a positive direction, gives rise to molecule  $R$ ,  $\frac{1}{2}b$  forwards; the equivalent molecule in the cell behind it is  $R_{\bar{b}}$ . The different parts of four molecules in the rest of the cell are of no concern in this discussion.

Comparison of Figs. 1 and 2 shows that the projection of greater area, the  $c$ -axis projection, has fewer resolved atoms than the smaller  $b$  projection. This is unusual, and unfortunate in that it lowers the accuracy attainable in the structure determination. It was because of the impossibility of independent observation of some atomic positions (notably  $\text{C}_2$ ,  $\text{C}_4$  and  $\text{C}_5$ ) that the bond lengths were used as a criterion for

Table 1. Atomic coordinates in molecule *P*

Values in brackets are of lower accuracy			
Atom	<i>x/a</i>	<i>y/b</i>	<i>z/c</i>
K <sup>+</sup>	0.465	0.828	0.035
C <sub>1</sub>	0.440	(0.162)	0.467
C <sub>2</sub>	0.383	0.242	0.560
C <sub>3</sub>	0.388	0.448	0.558
C <sub>4</sub>	(0.330)	(0.550)	(0.583)
C <sub>5</sub>	0.344	0.750	(0.537)
C <sub>6</sub>	0.286	0.840	0.558
O <sub>0</sub>	0.472	0.077	0.627
O <sub>1</sub>	0.449	(0.167)	0.227
O <sub>2</sub>	0.372	0.180	0.825
O <sub>3</sub>	0.435	0.509	0.702
O <sub>4</sub>	0.321	(0.545)	0.873
O <sub>5</sub>	0.361	0.772	0.268
O <sub>6</sub>	0.242	0.758	0.407

obtaining their coordinates. In addition the peak heights in Fig. 2 are sometimes not consistent. For instance those of C<sub>1</sub>, O<sub>4</sub> and O<sub>6</sub> are low, rendering their coordinates doubtful in this (*b*) projection, which, added to the uncertainty of C<sub>1</sub> and O<sub>4</sub> in the *c* projection (Fig. 1), makes their estimation difficult.

### Structure factors

In the structure-factor calculations Hartree's scattering factors for K<sup>+</sup>, O and C were used (*International Tables*, vol. 2, p. 571), no account being taken of the eleven hydrogen atoms. The final calculated structure factors were multiplied by a temperature factor,  $\exp[-B(\sin^2 \theta)/\lambda^2]$ : *B* for *hk0* was 1.09, and for *h0l* was 0.89. Three very small *h0l* terms were omitted from the final summation because their signs were still uncertain. No correction for termination-of-series errors was made.

The reflections *h00* are common to both *hk0* and *h0l*, but were observed with slightly different relative intensities. Also, where the *hk0* set contained an unreliable observation of the very strong near-in 200 reflection, the *h0l* had none, and the *hk0* value was used for both. No correction for the extinction of 200 was introduced, although its structure factor was calculated to be twice the observed value. The reflection 16,0,0, in spite of appearing weakly on the *h0l* photographs, was absent on the *hk0*'s. Its calculated value was so small, and of doubtful sign, that it was not included in the final summations. In both the electron-density summations the average of the two values of each *F*<sub>*h00*</sub> was used.

A comparison of the observed and calculated structure factors is listed in Table 2.\* Calculations of the

\* Table 2 has been withdrawn and deposited as Document No. 3981 with the ADI Auxiliary Publications Project, Photoduplication Service, Library of Congress, Washington 25, D.C., U.S.A. A copy may be secured by citing the document number and by remitting \$1.25 for photoprints, or \$1.25 for 35 mm. microfilm. Advance payment is required. Make checks or money orders payable to: Chief, Photoduplication Service, Library of Congress.

reliability index,  $R = \Sigma ||F_c| - |F_o|| / \Sigma |F_o|$ , gave good results, as follows:

	<i>hk0</i>	<i>h0l</i>
No. of reflections possible	226	154
No. of reflections observed	154	110
No. of reflections absent	72	44
Reflection of highest <i>h</i> index	30,0,0	30,0,0
Reflection of highest <i>k</i> or <i>l</i> index	10,9,0	11,0,6
<i>R</i> , with absences omitted	13.5%	15.2%
<i>R</i> , with absences and 200 omitted	12.7%	14.0%
<i>R</i> , with 200 omitted and absences included at one-half the smallest <i>F</i> <sub>0</sub>	17.3%	18.3%

The value of *F*<sub>000</sub> was calculated assuming 110 electrons per molecule instead of the 122 present in KC<sub>6</sub>O<sub>7</sub>H<sub>11</sub>; this excludes the eleven hydrogen atoms and the valence electron of the potassium atom.

The probable error in the coordinates was estimated to be about 0.02 Å, and that in the bond lengths about 0.04 Å.

### Description of the gluconate ion

The configuration found for the gluconate ion is completely in agreement with Fischer's representation, and seems acceptable chemically. It contains a six-membered zigzag carbon chain which is nearly planar. Thus there is no approximation to the ring present in glucose. The five hydroxyl oxygen atoms and two carboxylate oxygen atoms lie above and below the plane of the carbon atoms.

Bond lengths and angles are shown in Fig. 3, and

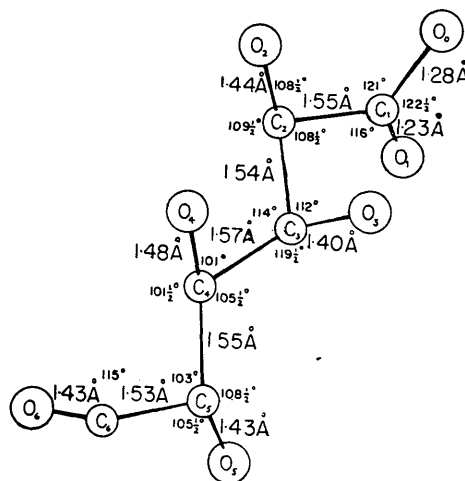


Fig. 3. Bond lengths and angles in the gluconate ion. Molecule *P* is viewed down the [011] axis. O<sub>0</sub> and O<sub>1</sub> are the carboxylate oxygen atoms.

the bond lengths are listed in Table 3. The C-C lengths lie between 1.53 Å and 1.57 Å, which is to be expected because the coordinates of some carbon atoms (C<sub>2</sub>, C<sub>4</sub> and C<sub>5</sub>) were chosen to give bond lengths near the standard length 1.54 Å.

The resulting angles are all close to tetrahedral, in the range 103–113°.



these octahedra related by crystal symmetry. In potassium sodium *dl*-tartrate tetrahydrate (Sadanaga, 1950), a potassium ion is coordinated to a completely irregular octahedron consisting of three oxygen atoms at about 2.7 Å and another three at about 3.5 Å. In contrast, the greater uniformity of the six K<sup>+</sup>-O bonds in potassium gluconate indicates its efficient packing.

Since each potassium ion is surrounded by four carboxylate oxygen atoms, each carboxylate group is bonded to four potassium ions, and each oxygen atom to two. In addition to these two ionic bonds, each carboxylate oxygen forms a hydrogen bond to a hydroxyl oxygen of another molecule, as illustrated in Fig. 5(a): O<sub>1</sub> is bonded to O<sub>2</sub> of the next molecule in the *c* direction, and O<sub>0</sub> is bonded to O<sub>3</sub> of the next molecule in the *b* direction through the ionic sheet. Each O<sub>0</sub> and O<sub>1</sub> thus has three external bonds, which presumably is possible because it has half a negative charge, giving it enough electronegativity to attract the slightly electropositive hydrogen atom nearby, as well as the potassium ions. The angles are not very far from the tetrahedral angle, and their distortion probably enables the molecules to pack more efficiently in the crystal. A similar tetrahedral configuration about a carboxylate oxygen atom could not be found in the literature.

Each hydroxyl group forms two external bonds, as expected, and the arrangement requires that the hydrogen atoms be in definite bonds. The hydrogen bonds link the molecules in nearly all directions (Fig. 4). It has been said already that O<sub>2</sub> of molecule *P* is bonded through its hydrogen atom to a carboxylate oxygen, O<sub>1</sub> of *P<sub>c</sub>*. In addition, O<sub>2</sub>(*P*) is bonded to O<sub>6</sub>(*Q*) in the *a* direction, using the H of O<sub>6</sub>. O<sub>6</sub>(*Q*) is also bonded to O<sub>4</sub>(*P*) in the *b* direction, using the H of O<sub>4</sub>. O<sub>4</sub>(*P*) makes its second bond to O<sub>5</sub>(*P<sub>c</sub>*) in the *c* direction, using the H of O<sub>5</sub>. Also O<sub>5</sub>(*P*) forms one apex of the coordination octahedron of potassium (*P*). O<sub>3</sub>(*P*), as has been described previously, uses its hydrogen atom to form a hydrogen bond to O<sub>0</sub>(*R*) in the *b* direction, and it forms an electrostatic bond to the same potassium ion to which O<sub>0</sub>(*P*) is bonded, R<sub>5</sub>.

All the distances between hydrogen-bonded oxygen atoms (Table 4) lie between 2.71 Å and 2.80 Å, in excellent agreement with other determinations. The angles that the OH-O bonds make with their C-O bonds vary from 99° to 134°, but two-thirds of them lie between 120° and 134°. The two C-O-O angles in pentaerythritol are 115° and 137° (Llewellyn, Cox & Goodwin, 1937); that in threonine is 120°.

Though some C-C and C-OH distances in the molecule were used to influence the determination of the coordinates of a few carbon atoms, no OH-O distances were used in this way. No assumptions were made initially about the hydrogen bonds, so there is little doubt that those found do represent the hydrogen bonding system in the crystal.

Molecule *P*, and molecule *Q* half a cell upwards in the *c* direction, are held together in the *a* and *b* directions by the hydrogen bonds O<sub>2</sub>-O<sub>6</sub> and O<sub>6</sub>-O<sub>4</sub>. *Q* is attached in the same way to *P<sub>c</sub>* in the next cell upwards. In addition each *P* and *Q* is joined to *P* and *Q* in the cell above by the hydrogen bonds O<sub>1</sub>-O<sub>2</sub>, and O<sub>4</sub>-O<sub>5</sub>. There is no link between two of these *PQ* columns in neighbouring cells in the *b* direction, except that they are both firmly held by ionic forces to the potassium sheets running throughout the crystal.

### The relation to α-glucose

The determination of the structure of α-glucose by McDonald & Beevers (1950, 1952) confirms that the sugar is a nearly flat pyranose ring in the Sachse *trans* form. It is interesting that the gluconate ion can be made to form the same ring very simply. If C<sub>2</sub>-C<sub>3</sub> and C<sub>3</sub>-C<sub>4</sub> are each twisted through a third of a turn, O<sub>1</sub> coincides with O<sub>5</sub>, and either then represents the ring oxygen atom. The result is that all the other oxygen atoms and the C<sub>6</sub>-O<sub>6</sub> bond, except of course O<sub>0</sub>, fall into their positions as described in the glucose structure. Though this manipulation of the molecular model is easy, it cannot be assumed that it is the mechanism of the opening and closing of the glucose ring in solution. However, it is possible that the primary result of these twists of the model, including the orientation of O<sub>0</sub>, is approximately the structure of δ-gluconolactone, which resembles the glucose ring in everything but the environment of C<sub>1</sub>.

I wish to thank the Women's Auxiliary of the Lanke-nau Hospital Research Institute for granting me a Fellowship to do this work, and the Fulbright Commission for a travel grant. My thanks are due also to Dr Seymour S. Cohen of the Children's Hospital of Philadelphia and the University of Pennsylvania, Philadelphia, for suggesting the subject. Above all, I am deeply grateful to Dr A. L. Patterson of the Institute for Cancer Research for his encouragement and advice at all times.

### References

- COHEN, S. S. (1951). *J. Biol. Chem.* **189**, 617.  
 FURBERG, S. (1950). *Acta Cryst.* **3**, 325.  
 KEENAN, G. H. & WEISBERG, S. M. (1929). *J. Phys. Chem.* **33**, 791.  
 LLEWELLYN, F., COX, E. G. & GOODWIN, T. H. (1937). *J. Chem. Soc.* p. 883.  
 McDONALD, T. R. R. & BEEVERS, C. A. (1950). *Acta Cryst.* **3**, 394.  
 McDONALD, T. R. R. & BEEVERS, C. A. (1952). *Acta Cryst.* **5**, 654.  
 PATTERSON, A. L. (1934). *Phys. Rev.* **46**, 372.  
 PATTERSON, A. L. (1935). *Z. Krystallogr.* **90**, 517.  
 PATTERSON, A. L. & TUNELL, G. (1942). *Amer. Min.* **27**, 655.  
 PEPINSKY, R. (1942). *Phys. Rev. A*, **61**, 726.  
 REHORST, K. (1928). *Ber. dtsch. chem. Ges. B*, **61**, 163.

- REHORST, K. (1930). *Ber. deutsch. chem. Ges. B*, **63**, 2279.  
 SADANAGA, R. (1950). *Acta Cryst.* **3**, 416.  
 SHOEMAKER, D. P., DONOHUE, J., SCHOMAKER, V. & COREY, R. B. (1950). *J. Amer. Chem. Soc.* **72**, 2328.  
 SKINNER, J. M. & SPEAKMAN, J. C. (1951). *J. Chem. Soc.* p. 185.  
 SPEAKMAN, J. C. (1949). *J. Chem. Soc.* p. 3357.  
 STERN, F. & BEEVERS, C. A. (1950). *Acta Cryst.* **3**, 341.

*Acta Cryst.* (1953). **6**, 781

## The Crystallography of Solid Dinitrogen Trioxide at $-115^{\circ}\text{C}$ .

BY THOMAS B. REED AND WILLIAM N. LIPSCOMB

*School of Chemistry, University of Minnesota, Minneapolis 14, Minnesota, U.S.A.*

(Received 30 March 1953)

The unit cell of  $\text{N}_2\text{O}_3$  crystals at  $-115^{\circ}\text{C}$ . is tetragonal with  $a = 16.4$ ,  $c = 8.86$  Å, and contains 32 molecules of  $\text{N}_2\text{O}_3$ . Complete  $hkl$  data from single crystals indicate that the space group is  $D_4^1-I4_12$ . The presence of an abnormally high decline of intensities with increasing angle of scattering, and the presence of a marked transition at roughly  $-125^{\circ}\text{C}$ ., suggest a disordered structure. Although the electron-density projection along  $c$  was refined to an agreement of  $R = 0.22$  (observed reflections only), an interpretation of this projection could not be made, and the structure remains unsolved.

### Introduction

An investigation of the structure of  $\text{N}_2\text{O}_3$  was undertaken because its enthalpy of dissociation (10.3 kcal./mole) is intermediate between that of  $\text{N}_2\text{O}_4$  (14.6 kcal./mole) and that of  $\text{N}_2\text{O}_2$  (4 kcal./mole). Since both  $\text{N}_2\text{O}_4$  (Broadley & Robertson, 1949) and  $\text{N}_2\text{O}_2$  (Dulmage, Meyers & Lipscomb, 1951) show anomalously long bonds, a similar anomaly was therefore expected for  $\text{N}_2\text{O}_3$ . However, as will be described, the presence of a probably disordered phase having a reasonably large, non-centrosymmetric unit cell has allowed us to determine only a partial structure of solid  $\text{N}_2\text{O}_3$ , and we have not obtained a chemically interesting interpretation of our results. However, it is to be expected that when calorimetric, magnetic susceptibility, spectroscopic, and other physical data are obtained for  $\text{N}_2\text{O}_3$ , interpretations of the diffraction data and electron-density map in terms of more complete crystal and molecular structures may become possible.

### Experimental

The general experimental techniques have been described elsewhere (Reed & Lipscomb, 1953), so that only those additional details pertaining to  $\text{N}_2\text{O}_3$  are described. Mixtures of NO and  $\text{NO}_2$  were sealed in capillaries about 1 mm. in diameter attached to thick pyrex bulbs about 10 mm. in diameter. As is indicated by the phase diagram (see Wilson & Bremner, 1948, p. 14) the liquid phase above  $-100^{\circ}\text{C}$ . contains excess  $\text{NO}_2$ , and probably for that reason our preliminary attempts to freeze the liquid yielded  $\text{N}_2\text{O}_4$  crystals.

However, when the sample was maintained at a few degrees above the melting point of about  $-100^{\circ}\text{C}$ . for a few hours to allow solution of the equilibrium amount of NO, good large single crystals were obtained, unfortunately always along with small fragments of other crystals. We feel sure that the easily recognizable reflections due to the fragments caused neither ambiguities in indexing nor errors in the intensity estimates. The characteristically larger areas of the reflections from the single crystal and the high symmetry of the diffraction photographs were very helpful in avoiding these ambiguities and errors. It must be remarked that single crystals of  $\text{N}_2\text{O}_3$  were many times more difficult to obtain than crystals of any substance so far studied in this laboratory. Unfortunately, the polarizing microscope was not useful for observation of the growth of crystals because of the opacity of the solid.

The crystals were maintained at  $-115 \pm 5^{\circ}\text{C}$ . during the photography. In the neighborhood of  $-125^{\circ}\text{C}$ . a major transition occurs. As the temperature is lowered the single-crystal reflections split up almost completely into a powder pattern.

The crystals, indicated by the diffraction patterns to be tetragonal, always grew with the  $c$  axis along the capillary. Consequently complete  $hkl$  data were obtained from precession photographs, all of which contained the  $00l$  reflections. In addition Weissenberg photographs were taken of the  $\{hkl0\}$  zone. Mo  $K\alpha$  radiation was used throughout. The integrated intensities of timed exposures on the precession photographs were measured by means of a Leeds and Northrup recording microdensitometer, and those on the Weissenberg photographs by means of visual estimates